SUPPLEMENTAL MATERIALS

MATERIALS & METHODS

Blood pressure measurements and echocardiographic assessment of left ventricular function

Systemic blood pressure (BP) was blindly determined in conscious mice by a non-invasive computerized tail-cuff method (CODA Kent Scientific) according to the manufacturer's instructions. For echocardiography, mice were anesthetized under gaseous anaesthesia (isoflurane-Vetflurane, Virbac 1.8-2% in a 1:1 mixture of oxygen:air). Hairs of the thoracic area were removed (hair-removing cream for sensitive skin), and the animal was positioned on a heating platform linked to the echography system (Vevo® 2100, VisualSonics) allowing the registration of ECG and respiratory rate. MS-550D (40 MHz) transducer was used for image acquisition; this transducer is specifically dedicated to mouse cardiac imaging (VisualSonics). Standard parameters were obtained using M-mode on "small-axis" views (SAX) and "long-axis" views. Parameters allowed the calculation of thickness of cardiac walls, ventricular volumes (during systole and diastole), estimated left ventricle mass, ejection fraction, fractional shortening, cardiac output and stroke volume.

Invasive right heart catheterization and assessment of pulmonary vascular changes

Mice were randomized and either studied in room air at 8-14 weeks of age, or were exposed to hypoxia (FiO_2=10%) for 3 weeks. At the end of these protocols, hemodynamic parameters were blindly measured in unventilated anesthetized mice (isoflurane) using a closed chest technique, by introducing a 1.4-F Millar catheter (ADInstruments, Paris, France) into the jugular vein and directing it to the right ventricle (RV) to assess the right ventricular systolic pressure (RVSP) [1-3]. Euthanasia was performed by exsanguination under isoflurane. The RV hypertrophy was calculated using the Fulton Index [weight ratio of right ventricle and (left ventricle + septum)] and the percentage of wall thickness [(2 × medial wall thickness/ external diameter) × 100] and of muscularized vessels were performed as previously described [3, 4]. The pulmonary circulation was flushed with 5mL of buffered saline at 37°C, and then the left lung was prepared for histological analyses and the right lung was quickly harvested, immediately snap-frozen in liquid nitrogen and kept at -80°C.

Microvessel perfusion

Fluorescent 45 µm microspheres (Polysciences, Inc) were injected into the left cardiac ventricle of anesthetized (isoflurane) to investigate left to right shunting (systemic arteriovenous shunts), or 15 µm microspheres (Life technologies) were injected intravenously to investigate pulmonary shunts in mice as previously described [5], Euthanasia was performed using an injection of pentobarbital 180 mg/kg, mice were dissected and fluorescent beads trapped in the tissue vasculature were examined using a Zeiss Axiobserver microscope.

Another group of animals was used to visualize the vasculature following perfusion with latex blue. Briefly, mice received a pentobarbital intraperitoneal injection (180 mg/kg). Abdominal and thoracic cavities were open, left and right atria were cut, the left ventricle was punctured with a 26-gauge needle, and a blue latex dye (Connecticut Valley Biological Supply Co.) was slowly and steadily injected. The vasculature was observed and organs of

interest were collected, rinsed in PBS and fixed with 10% formalin overnight at 4°C. Tissue clearing procedure was performed to enhance sample transparency and maximize delineation of the vascular casts using urea/Quadrol/Triton X-100 and triethanolamine/urea/sucrose solutions. Images were acquired using a Leica S8APO stereomicroscope.

RNA sequencing and real-time quantitative-PCR

Mouse lung tissue was flash frozen in liquid nitrogen and stored at -80°C. RNA extraction, RNA sample quality assessment, RNA library preparation, sequencing and raw data analysis were conducted at GENEWIZ, Inc. (South Plainfield, NJ, USA).

Total RNA was extracted from frozen tissue using the Qiagen RNeasy Plus Mini kit. RNA samples were quantified using Qubit 2.0 Fluorometer (Life Technologies, Carlsbad, CA, USA) and RNA integrity was checked with Agilent TapeStation (Agilent Technologies, Palo Alto, CA, USA).

rRNA depletion was performed using Ribozero rRNA Removal Kit (Illumina, San Diego, CA, USA). RNA sequencing library preparation used NEBNext Ultra RNA Library Prep Kit for Illumina by following the manufacturer's recommendations (NEB, Ipswich, MA, USA). Briefly, enriched RNAs were fragmented for 15 minutes at 94 °C. First strand and second strand cDNA were subsequently synthesized. cDNA fragments were end repaired and adenylated at 3'ends, and universal adapter was ligated to cDNA fragments, followed by index addition and library enrichment with limited cycle PCR. Sequencing libraries were validated using the Agilent Tapestation 4200 (Agilent Technologies, Palo Alto, CA, USA), and quantified by using Qubit 2.0 Fluorometer (Invitrogen, Carlsbad, CA) as well as by quantitative PCR (Applied Biosystems, Carlsbad, CA, USA).

The sequencing libraries were clustered on one lane of a flowcell. After clustering, the flowcell was loaded on the Illumina HiSeq 4000 instrument (or equivalent) according to manufacturer's instructions. The samples were sequenced using a 2x150 Paired End (PE) configuration. Image analysis and base calling were conducted by the HiSeq Control Software (HCS). Raw sequence data (.bcl files) generated from Illumina HiSeq was converted into fastq files and de-multiplexed using Illumina's bcl2fastq 2.17 software. One mis-match was allowed for index sequence identification.

After investigating the quality of the raw data, sequence reads were trimmed to remove possible adapter sequences and nucleotides with poor quality using Trimmomatic v.0.36. The trimmed reads were mapped to the the Mus musculus GRCm38 reference genome available on ENSEMBL using the STAR aligner v.2.5.2b. Gene counts were calculated from uniquely mapped reads using feature Counts from the Subread package v.1.5.2. Only unique reads that fell within exon regions were counted.

The gene hit counts table was then used for downstream differential expression analysis. A differential gene expression analysis between WT and DKO groups of samples was performed using the R-package DESeq2 (Wald test). Genes with adjusted p-values < 0.05 and absolute log2 fold changes > log2(1.5) were called as differentially expressed genes (DEG). A bi-clustering heatmap was used to visualize the expression profile of the top 40 differentially expressed genes with the lowest adjusted p-value by plotting their log2 transformed expression values in samples using the R-package pheatmap. A gene ontology analysis was performed on the statistically significant set of genes using DAVID functional annotation tool (https://david.ncifcrf.gov/summary.jsp). Gene Set Enrichment Analysis (GSEA) was performed on the full list of genes ranked by log2 fold change using the WEB-

based Gene SeT AnaLysis Toolkit (http://www.webgestalt.org/) with the functional database geneontology / Biological Process noRedundant.

We performed estimations of cell type abundances from our bulk lung transcriptomes using the method Cibertsortx [6]. To accomplish this, we used single-cell reference transcriptome profiles collected from mice lungs (Travaglini et al [7]). We filtered from these single-cell data the cell types identified by less than 40 cells, and generated a signature matrix composed of 10,000 cells sampled from the remaining cell types. This signature matrix was then used by Cibersortx, with S-mode batch correction, to predict cell type factions from our bulk lung transcriptomes. The heatmap showing cell type abundances per sample was produced with the pheamap function in R.

Level of lung mRNA level encoding endothelin-1 were measured by qRT-PCR according to the method previously described [3]. To assess the mRNA level of other genes, mRNA was extracted using an RNeasy kit (Macherey, Nagel), reverse transcription was performed using iScript kit from Biorad and quantitative PCR was performed using SsoAdvanced SYBR green kit from Biorad. The Delta-Delta Ct (**ΔΔ**Ct) method was used to obtain relative expression levels, normalized to *Rpl13a* levels. Primer sequences can be found in table S5.

Blood analysis, Western Blot, histology, and immunostaining

Whole blood or plasma was collected from 5-month-old mice. The total volume of blood collected via cardiac puncture was measured using a 2.5 mL graduated syringe. EDTA whole blood was analyzed using an XNL 550 automated hematology analyzer (Sysmex). Li-heparin plasma (collected after 4 hours of fasting) was analyzed using AU-480 automated clinical chemistry analyzer (Beckman Coulter). Concentrations of atrial natriuretic peptide (ANP), brain natriuretic peptide (BNP), endothelin (ET)-1 and of hyaluronic acid (HA) in plasma were evaluated using specific ELISA Kits from Ray Biotech for ANP and BNP and from R&D for all the others, according to the manufacturer instructions. ELISA for BMP9, BMP10 or for the heterodimer BMP9-BMP10 were performed as previously described [8].

Tissues were homogenized and sonicated in RIPA buffer containing protease and phosphatase inhibitors and 30 µg of protein was used to detect pSmad 1/5/8 (1/500, 13820 Cell Signaling), pSmad2/3 (1/200, 8828 Cell Signaling), and β-actin (1/400, A3854 Sigma).

Hematoxylin-Eosin (H&E; Sigma), Picrosirius red (Sigma) or Prussian blue (Merck) staining of the heart, lung, liver, spleen, and kidney tissues were performed using routine procedures. Images were acquired using Zeiss Axioplan or Axioscan microscopes and analyzed using Zen, Axiovision or Image J softwares. Cardiomyocyte size was determined by measuring the cross-sectional area of 100 cardiomyocytes in the left ventricular wall. Briefly, transverse heart sections (40-µm thickness) were blocked with PBS 3% BSA, stained with fluorescein conjugated Wheat Germ Agglutinin (WGA) (5 µg/mL, W834 Invitrogen) in PBS 1% BSA and with Hoechst (1/1000, 33342 Sigma) for nuclear counterstaining. Images were acquired with a Zeiss ApoTome microscope (objective x40) and analyzed using Zen software (Zeiss). Diameters of pulmonary capillary vessels were determined in semi-thin lung sections (500-nm thickness) stained with epoxy tissue stain (EMS). Briefly, 1-2 mm^3 pieces of lung tissue were fixed overnight in 2% glutaraldehyde at 4°C, post-fixed in Osmium buffer, dehydrated and embedded in epoxy resin (EMS). Sections were then stained and images were acquired using a Zeiss axiovision microscope and analyzed using Image J software.

Immunohistochemistry staining for alpha-smooth muscle actin (α-SM actin) were performed as previously described [3]. Briefly, lung sections (4-µm thickness) were deparaffined and stained with (HE), or incubated with

retrieval buffer. Then, sections were saturated with blocking buffer and incubated overnight with α-SM actin antibodies (1:200, sc32251, Santa Cruz), followed by corresponding secondary fluorescent-labeled antibodies (Thermo Fisher Scientific). Nuclei were labelled using DAPI (Thermo Fisher Scientific). Mounting was performed using ProLong Gold antifade reagent (Thermo Fisher Scientific). All images were taken using a LSM700 confocal microscope (Zeiss, Marly-le-Roi, France).

Chick Chorioallantoic Membrane (CAM) assay

Fertilized Gallus gallus (Chicken) eggs were incubated at 37°C in a 65% humidified environment. They were rotated during 3 days (25° every 4h). On day 3, a window was created in the eggshell and sealed with medical tape. On day 10, a plastic ring (made from Nunc Thermanox coverslips) was placed on the surface of the CAM in each egg and received 50 µL of control vehicle (PBS BSA 0.1% DMSO 0.5%) or treatment solution containing 50 or 500 µM of Bosentan (R&D), 50 or 500 µM of Captopril (Tocris) or 0.5, 50 or 500 µM of Terguride (Abcam) in association with 20 nM of BMP9 (R&D) or not. The CAM was observed and imaged under a macroscope (AZ-100 multizoom, Nikon) after 4h and 24h of treatment. After 24h of treatment, 100 µL of FITC-Dextran solution was injected into the CAM vessels. Fluorescence images were taken using the 2X objective of the macroscope and automated quantification of the area of FITC positive vessels within the rings was performed using Angiotool software.

SUPPLEMENTARY FIGURE LEGENDS

Figure S1: BMP9, BMP10 and BMP9-BMP10 heterodimer concentration in mouse plasma measured by ELISA (n=8-10 mice/group). (**a**) *Bmp9* and *Bmp10* mRNA levels in liver (**b**) heart (right atria) (**c**) and lungs (**d**), normalized to *Rpl13a*. Data are presented as mean ± SEM of n=8-10 male mice per group and analyzed using a Kruskal Wallis test followed by a Dunn's test. *p<0.05, **p<0.01, ***p<0.001, ****p<0.0001 vs WT

Figure S2: Combined loss of *Bmp9* and *Bmp10* leads to cardiomegaly and splenomegaly for both male and female mice. Body weight, femur length and weight of the heart, liver, kidney and spleen of male (**a**) and female (**b**) mice. All mice were injected with tamoxifen at the age of 2 months and sacrificed at the age of 5 months. Data are presented as mean ± SEM of n=9-11 mice/group and analyzed using a Kruskall Wallis test followed by a Dunn's test. **p<0.01, ****p<0.0001 vs WT. #p<0.05; ##p<0.01, ###p<0.001 vs Bmp9-KO. $p<0.05; $$p<0.01 vs Bmp10-cKO.

Figure S3: Weight of the right ventricle (RV) (**a**) or left ventricle + septum (LV+S) (**b**) from WT and DKO mice (n=6-7/group). Data are presented as mean ± SEM and analyzed using a Mann-Whitney test. **p<0.01 vs WT. Representative photomicrographs of spleen sections stained with hematoxylin and eosin, scale bar 500 µm (**c**) and of liver sections stained with Picrosirius red, scale bar 100 µm (**d**). Quantitative analysis of the percentage area of liver sections stained in red (**e**). Plasma concentration of hyaluronic acid (HA) determined by ELISA (**f**). All mice were injected with tamoxifen at the age of 2 months and sacrificed at the age of 5 months. Data are presented as mean ± SEM of n=4-8 mice/group and analyzed using a Kruskal Wallis test followed by a Dunn's test. *p<0.05 vs WT. .#p<0.05 vs Bmp9-KO.

Figure S4: Relative mRNA levels of *Acvrl1, Eng, Bmpr2, Id1, Smad6,* in lung (**a**), liver (**b**) right atria (**c**) and left ventricle (**d**), normalized to *Rpl13a*. Representative western blots and quantitative analysis of pSmad1/5/8 and pSmad2/3 protein level in lung tissue, normalized to β-actin levels (**e**) Data are presented as mean ± SEM of n=6-10 male mice per group and analyzed using a Kruskal Wallis test followed by a Dunn's test. *p<0.05, **p<0.01, ****p<0.0001 vs WT

Figure S5: No obvious signs of cardiac fibrosis were observed after deletion of *Bmp9* and/or *Bmp10*. Heart sections stained with Picrosirius red represented as a mosaic of photomicrographs to show the entire section, scale bar 200 µm (**a**) or single photomicrographs, scale bar 100 µm (**b**). Mice were injected with tamoxifen at the age of 2 months and sacrificed at the age of 4 months. n=4/group

Figure S6: Representative photomicrographs of clarified intestines (**a**) and brains (**b**) from latex blue WT and DKO injected mice (n=4-6/group). Extracted blood volume of WT, Bmp9-KO, Bmp10-cKO and DKO mice (n=11-14 mice/group) (**c**). Data are presented as mean ± SEM and analyzed using a Kruskal Wallis test followed by a Dunn's test. **p<0.01 vs WT, #p<0.05 vs Bmp9-KO. $$p<0.01 vs Bmp10-cKO (**c**). Representative photomicrographs of the thyroid gland (**d**) of WT and DKO mice (n=8/group). All mice were injected with tamoxifen at the age of 2 months and sacrificed at the age of 4-5 months. Scale bar 1mm.

Figure S7: RNAseq analysis was performed on lung tissue from n=5 WT and n=7 DKO mice that were injected with tamoxifen at the age of 2 months and sacrificed at the age of 5 months. Genes with adjusted p-values < 0.05 and absolute log2 fold changes > log2(1.5) were called as differentially expressed genes (DEG). A gene ontology analysis was performed on these DEG using DAVID functional annotation tool (https://david.ncifcrf.gov/summary.jsp). Enriched gene ontologies sorted by modified Fisher Exact p-value (EASE score) were plotted, each data point in the dot plot represents a gene ontology, the -log10 p-value is on the x-axis, the size of the dot represents the number of DEG and the color scale the percentage of DEG involved in the gene ontology term.

Figure S8: Relative mRNA levels (normalized to *Rpl13a*) of *Ccl2, Ccl3, Cxcl5* from lung (**a**) and of *Tbx20, Nkx2-5* from left ventricle (**b**). Data are presented as mean ± SEM of n=6-10 male mice per group and analyzed using a Kruskal Wallis test followed by a Dunn's test. *p<0.05, **p<0.01 vs WT

Heatmap of predicted percentages of the different cell types in lungs from WT and DKO mice (n=5 WT and n=7 DKO mice per group) obtained using Cibersortx tool (**c**). Cell type abundances that were significantly different in DKO vs WT mice were visualized using bar plots (**d**). Data are presented as mean ± SEM and analyzed using a Mann-Whitney test *p<0.05, **p<0.01 vs WT.

Figure S9: Representative photomicrographs and quantitative analysis of FITC-Dextran injected blood vessels from chick chorioallantoic membranes treated with captopril (Capt) at 0, 50 and 500 µM, or terguride (Ter) at 0.5, 50 and 500 µM in combination with BMP9 (20 nM) or not for 24 hours. Scale bar 250 µm. For captopril treated eggs, data are presented as mean ± SEM of n=3-4 eggs/condition and analyzed using a Mann Whitney test. *p<0.05 vs captopril treated condition without BMP9. For terguride treated eggs automated quantitative analysis was not possible for several eggs due to high background and mortality at 24h, therefore no statistical analysis was performed.

SUPPLEMENTARY TABLES

Table S1: Clinical chemistry and metabolic exploration. Biochemical analysis of plasma from n=6 WT, n=8 *Bmp9*-KO, n=5 *Bmp10*-cKO and n=7 DKO mice. All mice were injected with tamoxifen at the age of 2 months and blood was collected at the age of 5 months. LDH = lactate dehydrogenase, AST = aspartate aminotransferase, ALT = alanine aminotransferase.

		WT		***Bmp9*-KO**		***Bmp10*-cKO**		**DKO**	
		MEAN	SEM	**MEAN**	SEM	**MEAN**	SEM	**MEAN**	SEM
Glucose	**mmol/l**	**16.68**	1.53	**15.04**	1.32	**17.00**	0.64	**12.23**	1.37
Urea	**mmol/l**	**7.37**	0.40	**6.61**	0.40	**7.18**	0.38	**7.01**	0.40
Sodium	**mmol/l**	**152.17**	0.60	**150.63**	0.65	**149.80**	0.20	**152.43**	0.84
Potassium	**mmol/l**	**4.57**	0.19	**5.29**	0.39	**4.38**	0.20	**4.99**	0.31
Chloride	**mmol/l**	**113.00**	0.93	**113.88**	0.58	**112.60**	0.68	**115.43**	1.27
Total proteins	**g/l**	**49.33**	0.84	**48.88**	0.74	**48.60**	0.60	**46.71**	1.15
Albumin	**g/l**	**27.33**	0.49	**27.13**	0.69	**27.20**	0.20	**25.29**	0.92
Calcium	**mmol/l**	**2.18**	0.01	**2.15**	0.01	**2.14**	0.02	**2.12**	0.02
Phosphorus	**mmol/l**	**2.14**	0.10	**2.03**	0.13	**1.95**	0.10	**2.51**	0.19
Total bilirubin	**µmol/l**	**3.18**	0.88	**4.11**	1.25	**2.16**	0.23	**3.44**	1.02
Creatine kinase	**U/l**	**159.33**	70.35	**162.00**	122.83	**155.40**	25.42	**104.86**	22.22
LDH	**U/l**	**683.17**	209.29	**569.71**	132.23	**465.80**	113.35	**637.29**	108.10
AST	**U/l**	**99.83**	21.77	**89.86**	19.38	**101.60**	9.42	**90.71**	13.58
ALT	**U/l**	**46.00**	15.74	**23.71**	5.63	**44.20**	7.30	**18.86**	5.29
ALP	**U/l**	**61.33**	3.96	**66.88**	7.73	**51.80**	3.62	**53.71**	3.98
Total cholesterol	**mmol/l**	**3.10**	0.31	**2.61**	0.24	**3.09**	0.15	**2.48**	0.18
Triglyceride	**mmol/l**	**0.60**	0.06	**0.48**	0.03	**0.57**	0.06	**0.46**	0.04
Creatinine	**µmol/l**	**8.33**	0.49	**9.00**	1.48	**7.40**	0.51	**7.86**	0.34

Table S2: Hematological analysis. All mice were injected with tamoxifen at the age of 2 months and blood was collected at the age of 5 months (n=5 WT, n=6 *Bmp9*-KO, n=5 *Bmp10*-cKO and n=7 DKO mice). WBC = white blood cells, RBC = red blood cells, HGB = hemoglobin, HCT = hematocrit, MCV = mean corpuscular volume, MCH = mean corpuscular hemoglobin, MCHC = mean corpuscular hemoglobin concentration, PLT = platelets, MPV = mean platelet volume

		WT		***Bmp9*-KO**		***Bmp10*-KO**		**DKO**	
		MEAN	SEM	**MEAN**	SEM	**MEAN**	SEM	**MEAN**	SEM
WBC	$x10^3$ cells/µL	**15.70**	0.96	**16.59**	1.58	**16.34**	1.32	**15.35**	1.27
RBC	$x10^6$ cells/µL	**10.67**	0.40	**9.09**	0.26	**10.76**	0.18	**9.04**	0.29
HGB	g/dL	**15.36**	0.45	**13.33**	0.32	**15.48**	0.32	**13.63**	0.54
HCT	%	**50.38**	1.42	**44.53**	1.12	**51.42**	1.06	**45.00**	1.53
MCV	fL	**47.26**	0.52	**49.02**	0.76	**47.78**	0.31	**49.77**	0.77
MCH	pg	**14.42**	0.13	**14.68**	0.19	**14.38**	0.07	**15.06**	0.31
MCHC	g/dL	**30.46**	0.11	**29.63**	0.39	**30.10**	0.10	**30.24**	0.22
PLT	$x10^3$ cells/µL	**826.40**	62.84	**711.00**	92.20	**748.25**	43.47	**534.14**	75.61
MPV	fL	**6.66**	0.05	**6.78**	0.09	**6.70**	0.05	**6.84**	0.07

225 Table S3: Selection of enriched gene ontology terms and associated differentially expressed genes represented in
226 figure S7

GO number	GO term	Count	%	PValue	DEG
GO:0006954	inflammatory response	34	6.75	1.06E-12	CXCL1, C3AR1, CCL3, CXCL5, TNFRSF26, CXCL3, CCR1, PTGS1, CXCL2, CCL9, FPR1, CCL8, MMP25, CCL6, SLC11A1, CHIL4, CCL22, NAIP2, CHIL1, CCL20, CHIL3, ZC3H12A, SPP1, LIPA, OLR1, TLR13, CHST4, CCL17, PRKCQ, TNFRSF9, PLA2G7, TRP73, CLEC7A, BMPR1B
GO:0007155	cell adhesion	28	5.56	9.12E-06	CADM3, CADM2, PCDH20, ITGAE, ITGB2, IGSF11, ITGAX, FAT3, TNR, GPNMB, SPP1, KIRREL3, TYRO3, CLCA2, OLR1, BMX, ACKR3, TINAGL1, CD84, LAMA1, LYVE1, ITGA6, DSG2, FREM2, FREM1, CD33, RELN, ADAM15
GO:0030574	collagen catabolic process	7	1.39	1.01E-05	CTSK, MMP8, MMP19, MMP16, CTSS, MMP13, ADAM15
GO:0070374	positive regulation of ERK1 and ERK2 cascade	15	2.98	6.91E-05	CCL3, CCR1, CCL9, CCL8, ACKR3, ESR2, CCL6, CCL17, CCL22, CCL20, CHIL1, TREM2, GPNMB, HTR2B, HTR2A
GO:0007204	positive regulation of cytosolic calcium ion concentration	12	2.38	4.15E-04	CXCL1, C3AR1, CCKAR, GNA15, CCL3, P2RY2, CCR1, CXCL3, CXCL2, EDN1, FPR1, HTR2A
GO:0022617	extracellular matrix disassembly	5	0.99	0.0012	SH3PXD2B, LAMA1, MMP19, MMP13, MMP12
GO:0014065	phosphatidylinositol 3-kinase signaling	5	0.99	0.0020	EDN1, IGF1, PIK3R5, HTR2B, HTR2A
GO:0055072	iron ion homeostasis	6	1.19	0.0021	LCN2, SLC11A1, STEAP4, EPB42, SLC40A1, B2M
GO:0045766	positive regulation of angiogenesis	9	1.79	0.0051	VEGFC, C3AR1, GDF2, LGALS3, CHIL1, PGF, LRG1, ZC3H12A, ITGB2
GO:0003341	cilium movement	5	0.99	0.0069	DNAH11, DNAH7B, HYDIN, DNAH5, DNAH6
GO:0006811	ion transport	23	4.56	0.0096	KCNH1, STEAP4, CLCA2, SLC6A15, CFTR, KCNJ10, SLCO2B1, FXYD6, KCNK2, LRRC26, LCN2, SLC11A1, ATP2B2, SLC23A1, TTYH2, KCNN3, SLC4A1, SLC38A1, SLC40A1, ATP6V0D2, SLC4A5, GRID1, GABRP
GO:0030335	positive regulation of cell migration	11	2.18	0.0142	C3AR1, IGF1R, SEMA6B, CCL3, PLET1, ITGA6, TIAM1, CCR1, EDN1, IGF1, GPNMB
GO:0007229	integrin-mediated signaling pathway	7	1.39	0.0162	NME2, ITGAX, ITGA6, ADAMTS20, ITGAE, ITGB2, ADAM15
GO:0001525	angiogenesis	12	2.38	0.0164	VEGFC, GDF2, OVOL2, PGF, LEPR, MMP19, ZC3H12A, ACKR3, TNFAIP2, VASH1, MMRN2, ADAM15
GO:0007599	hemostasis	5	0.99	0.0178	ANXA8, PROZ, F8, SERPIND1, F7
GO:0030073	insulin secretion	4	0.79	0.0404	CCKAR, IL1RN, FFAR1, PCLO
GO:0008217	regulation of blood pressure	5	0.99	0.0465	C3AR1, NPY, PTGS1, EDN1, DLL1
GO:0001938	positive regulation of endothelial cell proliferation	5	0.99	0.0588	VEGFC, GDF2, PGF, LRG1, HTR2B
GO:0007275	multicellular organism development	31	6.15	0.0673	DHH, TNFRSF26, PGF, PAX5, OVOL2, FAT3, ZC3H12A, LHX6, UNC5D, TCF23, NGEF, ZFP423, MMP19, ACKR3, DLL1, SIX4, VEGFC, TNFRSF9, SEMA6B, HOXD8, m, NXN, FREM2, DBP, FREM1, GADD45G, WIF1, RELN, TNFAIP2, GAP43, KIF26B
GO:0045907	positive regulation of vasoconstriction	4	0.79	0.0749	TBXAS1, SMAD6, PTGS1, HTR2A

227
228

229

Table S4: Lists of GO enriched terms and associated differentially expressed genes represented in figure 4b. Downregulated genes are represented in blue and upregulated genes are represented in blue.

category	GO number	GO term	Nb of DEG	DEG
inflammation / immune response	GO:0006954 GO:0070098 GO:0030593 GO:0006955 GO:0071346 GO:0006935 GO:0071347 GO:0060326 GO:0002376 GO:0002548 GO:0048247 GO:0071356 GO:0045087 GO:0035458 GO:0090023 GO:2000660 GO:2001180	inflammatory response chemokine-mediated signaling pathway neutrophil chemotaxis immune response cellular response to interferon-gamma chemotaxis cellular response to interleukin-1 cell chemotaxis immune system process monocyte chemotaxis lymphocyte chemotaxis cellular response to tumor necrosis factor innate immune response cellular response to interferon-beta positive regulation of neutrophil chemotaxis negative regulation of interleukin-1-mediated signaling pathway negative regulation of interleukin-10 secretion	82	CXCL1, MRC1, C3AR1, LCN2, ADGRE1, CCL22, LGALS3, GBP6, IL1R2, CD84, CCL3, PRKCQ, OLR1, TLR13, F830016B08RIK, IL1RN, TNFRSF9, CXCL5, TNFRSF26, CCL20, BMX, IIGP1, CXCL3, CCR1, CXCL2, VPREB3, STAR, LILRB4A, CCL9, CCL8, OAS2, TGTP2, EDN1, CHIL1, MALT1, TGTP1, CCL6, TRIM10, GM4951, FPR1, H2-Q7, CCL17, FCGR1, FCGR3, IL12B, ZC3H12A, B2M, ACKR3, C1QA, PTGS1, ITGB2, SUSD2, CLEC4N, CXCR1, MMP25, SLC11A1, CHIL4, NAIP2, CHIL3, SPP1, LIPA, CHST4, PLA2G7, TRP73, CLEC7A, BMPR1B, ACKR4, IGF1R, NFIL3, SMAD6, CTSS, TINAGL1, C1QB, CD300A, SERPINA3G, CD300LF, CLEC4D, CLEC5A, CD300LD, OAS1A, TREM2, ADAM15
ion transport	GO:0007204 GO:0051928 GO:0006811	positive regulation of cytosolic calcium ion concentration positive regulation of calcium ion transport ion transport	38	KCNH1, STEAP4, CLCA2, SLC6A15, CFTR, KCNJ10, SLCO2B1, FXYD6, KCNK2, LRRC26, LCN2, SLC11A1, ATP2B2, SLC23A1, TTYH2, KCNN3, SLC4A1, SLC38A1, SLC40A1, ATP6V0D2, SLC4A5, GRID1, GABRP, CXCL1, C3AR1, CCKAR, GNA15, CCL3, P2RY2, CCR1, CXCL3, CXCL2, EDN1, FPR1, HTR2A, ATP2B2, FFAR1, LPAR3
ECM disassembly	GO:0030574 GO:0006508 GO:0022617	collagen catabolic process proteolysis extracellular matrix disassembly	30	DHH, RBP3, MMP8, MMP25, PROZ, DPP6, PCSK5, CLCA2, ADAMTS20, MMP19, MMP17, MMP16, MALT1, CTSS, F7, TINAGL1, MMP13, MMP12, CTSK, CTSD, RELN, PRSS23, PHEX, ADAMDEC1, ADAM15, ASPRV1, ADAMTS4, CTSK, SH3PXD2B, LAMA1
adhesion	GO:0007155 GO:0007229	cell adhesion integrin-mediated signaling pathway	30	CADM3, CADM2, PCDH20, ITGAE, ITGB2, IGSF11, ITGAX, FAT3, TNR, GPNMB, SPP1, KIRREL3, TYRO3, CLCA2, OLR1, BMX, ACKR3, TINAGL1, CD84, LAMA1, LYVE1, ITGA6, DSG2, FREM2, FREM1, CD33, RELN, ADAM15, NME2, ADAMTS20
angiogenesis	GO:0045766 GO:0001525 GO:0001938	positive regulation of angiogenesis angiogenesis positive regulation of endothelial cell proliferation	18	VEGFC, C3AR1, GDF2, LGALS3, CHIL1, PGF, LRG1, ZC3H12A, ITGB2, OVOL2, LEPR, MMP19, ACKR3, TNFAIP2, VASH1, MMRN2, ADAM15, HTR2B
blood pressure / vasoreactivity	GO:0045019 GO:0007200 GO:0008217 GO:0045907	negative regulation of nitric oxide biosynthetic process phospholipase C-activating G-protein coupled receptor signaling pathway regulation of blood pressure positive regulation of vasoconstriction	14	GLA, ACP5, ZC3H12A, C3AR1, GNA15, P2RY2, FPR1, HTR2A, NPY, PTGS1, EDN1, DLL1, TBXAS1, SMAD6

233 Table S5. List of Primer

234 Primers for quantitative RT-PCR were designed using Primer-Blast on GenBank sequences and are separated by
235 at least one intron or span an exon-exon junction for intron containing genes.

Gene	GenBank sequences	Forward (5'-3')	Reverse (5'-3')
Rpl13a	NM_009438.5	CCCTCCACCCTATGACAAGA	TTCTCCTCCAGAGTGGCTGT
Id1	NM_010495.3	CGCTCAGCACCCTGAACGGC	TCCGGTGGCTGCGGTAGTGT
Acvlr1	NM_009612.3	CCTCACGAGATGAGCAGTCC	GGCGATGAAGCCTAGGATGTT
Bmpr2	NM_007561.4	TGGCAGTGAGGTCACTCAAG	TTGCGTTCATTCTGCATAGC
Eng	NM_001146348.1	GCCAAAGTGTGGCAATCAGG	TGGTCGTCAGTGTCTTCAGC
Bmp10	NM_009756.3	TCCATGCCGTCTGCTAACATCATC	ACATCATGCGATCTCTCTGCACCA
Smad6	NM_008542.3	CTGCGGGCCAGAATCACCGC	GCTCGGCTTGGTGGCATCCG
Edn-1	NM_010104.4	GGCCCAAAGTACCATGCAGA	TGCTATTGCTGATGGCCTCC
Nkx2-5	NM_008700.2	GACCCTCGGGCGGATAAAAA	CCATCCGTCTCGGCTTTGT
Tbx20	NM_194263.2	GTTTGCCAAAGGATTCCGGG	CCGGGCATAGGAATGCTTCT
Cxcl5	NM_009141.3	CGGTTCCATCTCGCCATTCA	GCTATGACTGAGGAAGGGGC
Ccl3	NM_011337.2	ATATGGAGCTGACACCCCGA	AGCAAAGGCTGCTGGTTTCA
Ccl2	NM_011333.3	CTGCATCTGCCCTAAGGTCT	AGTGCTTGAGGTGGTTGTGG
Bmp9 (Gdf-2)	NM_019506.4	CAATGACCGCAGCAATGGG	AAGCATGGTCTCCTGCTCAT

236

237

SUPPLEMENTARY REFERENCES

1. Guignabert C, Alvira CM, Alastalo TP, Sawada H, Hansmann G, Zhao M, Wang L, El-Bizri N, Rabinovitch M. Tie2-mediated loss of peroxisome proliferator-activated receptor-gamma in mice causes PDGF receptor-beta-dependent pulmonary arterial muscularization. *Am J Physiol Lung Cell Mol Physiol* 2009;**297**:L1082-1090.
2. Guignabert C, Izikki M, Tu LI, Li Z, Zadigue P, Barlier-Mur AM, Hanoun N, Rodman D, Hamon M, Adnot S, Eddahibi S. Transgenic mice overexpressing the 5-hydroxytryptamine transporter gene in smooth muscle develop pulmonary hypertension. *Circ Res* 2006;**98**:1323-1330.
3. Tu L, Desroches-Castan A, Mallet C, Guyon L, Cumont A, Phan C, Robert F, Thuillet R, Bordenave J, Sekine A, Huertas A, Ritvos O, Savale L, Feige J-J, Humbert M, Bailly S, Guignabert C. Selective BMP-9 Inhibition Partially Protects Against Experimental Pulmonary Hypertension. *Circulation Research* 2019;**124**:846-855.
4. Bordenave J, Thuillet R, Tu L, Phan C, Simonneau G, Huertas A, Hibert M, Bonnet D, Humbert M, Frossard N, Guignabert C. Neutralization of CXCL12 reverses established pulmonary hypertension in the sugen-hypoxia rat model. *Eur Respir J* 2017;**50**:PA2385.
5. Tual-Chalot S, Garcia-Collado M, Redgrave RE, Singh E, Davison B, Park C, Lin H, Luli S, Jin Y, Wang Y, Lawrie A, Jakobsson L, Arthur HM. Loss of Endothelial Endoglin Promotes High-Output Heart Failure Through Peripheral Arteriovenous Shunting Driven by VEGF Signaling. *Circ Res* 2020;**126**:243-257.
6. Newman AM, Steen CB, Liu CL, Gentles AJ, Chaudhuri AA, Scherer F, Khodadoust MS, Esfahani MS, Luca BA, Steiner D, Diehn M, Alizadeh AA. Determining cell type abundance and expression from bulk tissues with digital cytometry. *Nat Biotechnol* 2019;**37**:773-782.
7. Travaglini KJ, Nabhan AN, Penland L, Sinha R, Gillich A, Sit RV, Chang S, Conley SD, Mori Y, Seita J, Berry GJ, Shrager JB, Metzger RJ, Kuo CS, Neff N, Weissman IL, Quake SR, Krasnow MA. A molecular cell atlas of the human lung from single-cell RNA sequencing. *Nature* 2020;**587**:619-625.
8. Tillet E, Ouarne M, Desroches-Castan A, Mallet C, Subileau M, Didier R, Lioutsko A, Belthier G, Feige JJ, Bailly S. A heterodimer formed by bone morphogenetic protein 9 (BMP9) and BMP10 provides most BMP biological activity in plasma. *J Biol Chem* 2018;**293**:10963-10974.

Figure S1

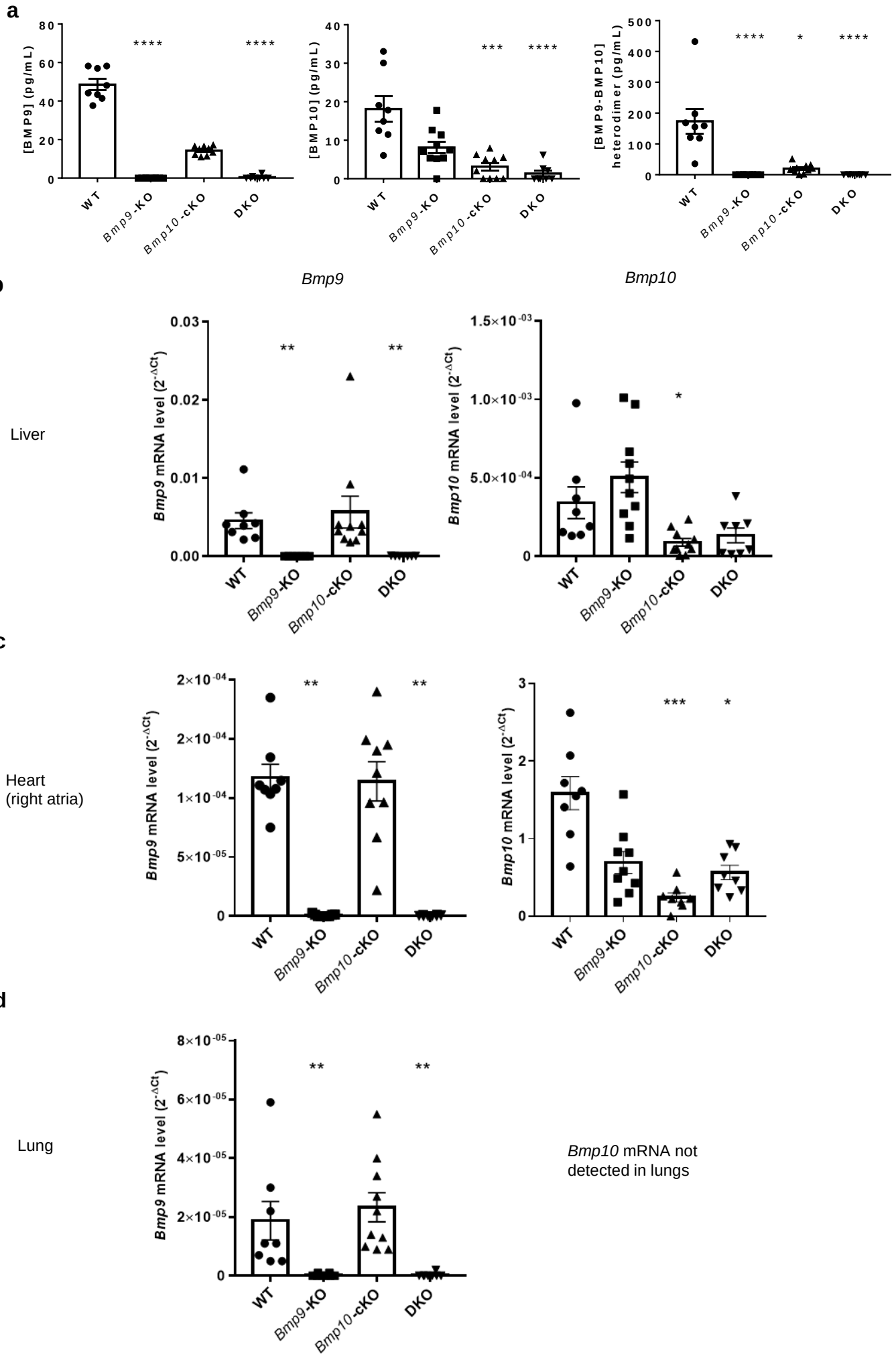
a
[BMP9] (pg/mL)
[BMP10] (pg/mL)
[BMP9-BMP10] heterodimer (pg/mL)
WT
Bmp9-KO
Bmp10-cKO
DKO
b
Bmp9
Bmp10
Liver
Bmp9 mRNA level (2^-ΔCt)
Bmp10 mRNA level (2^-ΔCt)
c
Heart (right atria)
d
Lung
Bmp10 mRNA not detected in lungs

Figure S2

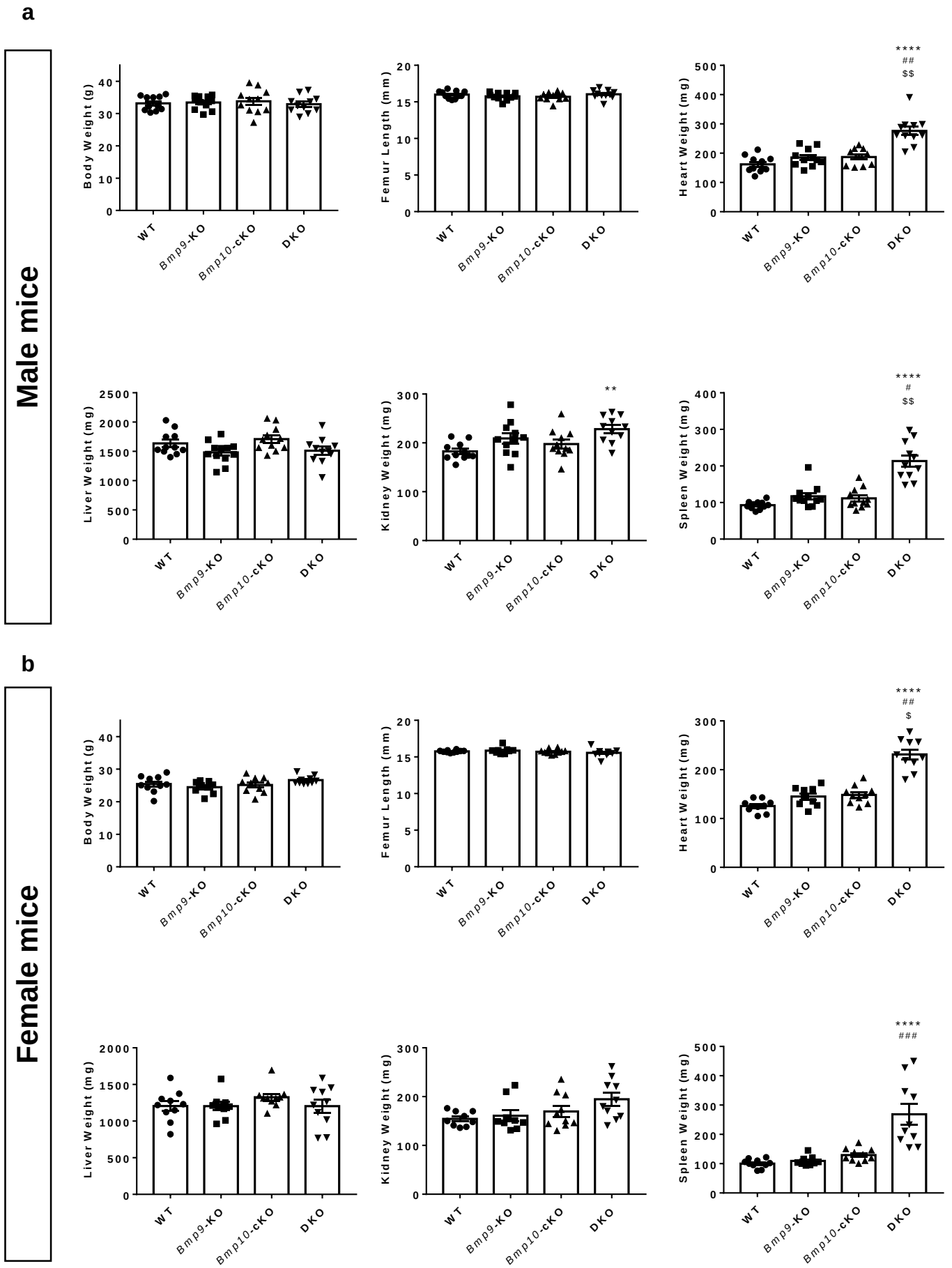
a
Male mice
Body Weight (g)
Femur Length (mm)
Heart Weight (mg)
Liver Weight (mg)
Kidney Weight (mg)
Spleen Weight (mg)
WT
Bmp9-KO
Bmp10-cKO
DKO
b
Female mice
Body Weight (g)
Femur Length (mm)
Heart Weight (mg)
Liver Weight (mg)
Kidney Weight (mg)
Spleen Weight (mg)
WT
Bmp9-KO
Bmp10-cKO
DKO

Figure S3

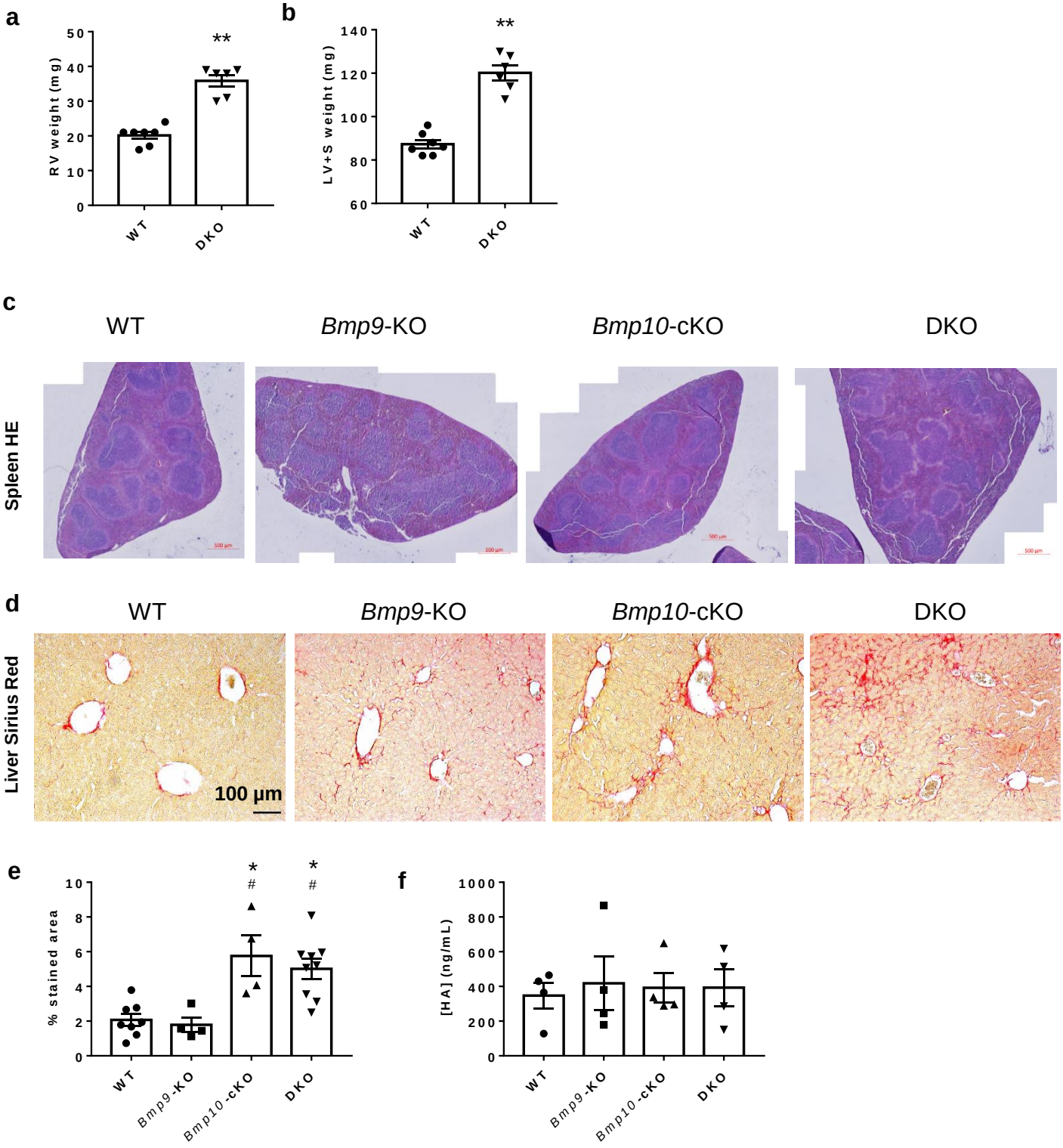
a
RV weight (mg)
50
40
30
20
10
0
**
WT
DKO
b
LV+S weight (mg)
140
120
100
80
60
**
WT
DKO
c
WT
Bmp9-KO
Bmp10-cKO
DKO
Spleen HE
d
WT
Bmp9-KO
Bmp10-cKO
DKO
Liver Sirius Red
100 µm
e
% stained area
10
8
6
4
2
0
*
#
*
#
WT
Bmp9-KO
Bmp10-cKO
DKO
f
[HA] (ng/mL)
1000
800
600
400
200
0
WT
Bmp9-KO
Bmp10-cKO
DKO

Figure S4

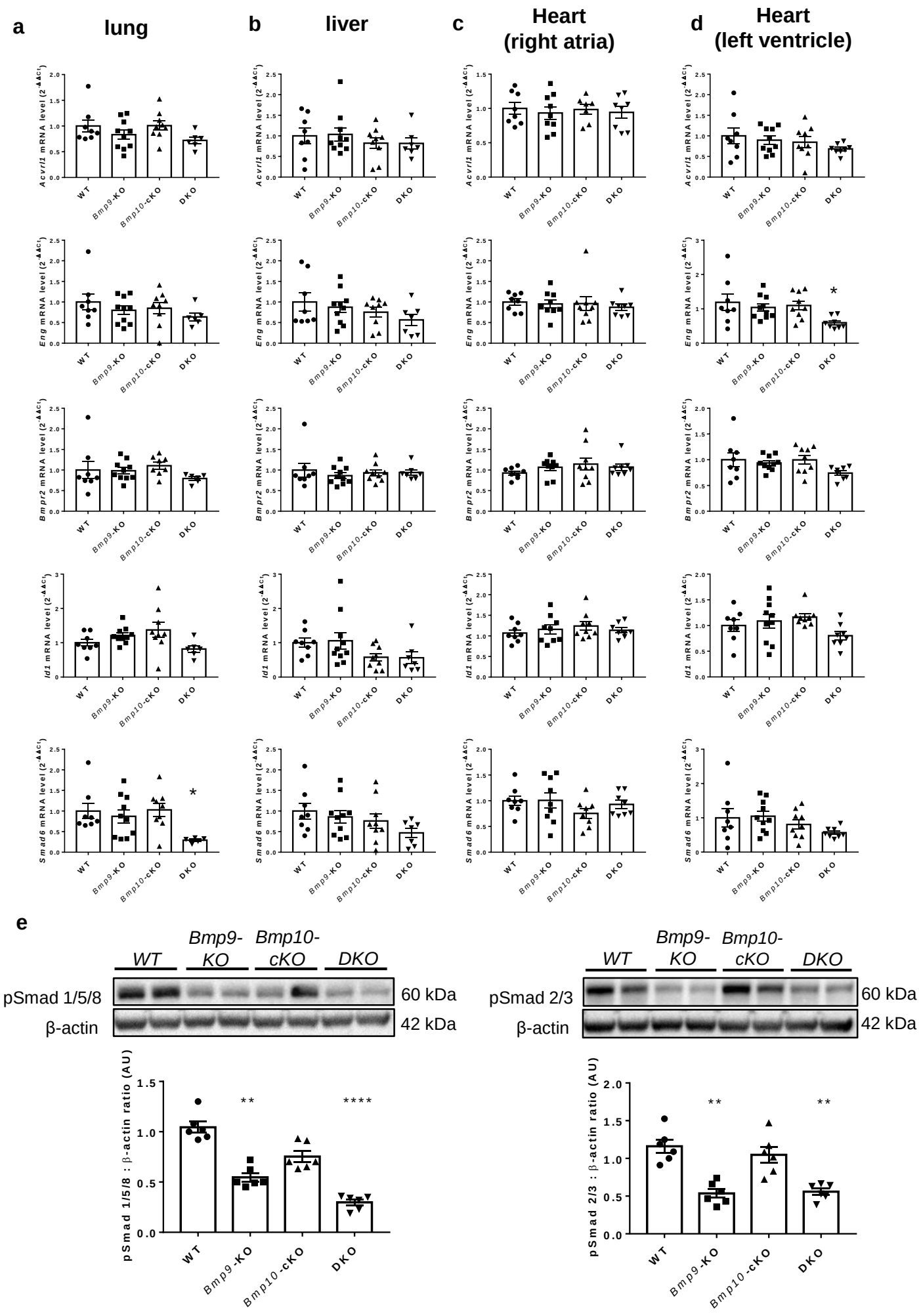
a
lung
b
liver
c
Heart (right atria)
d
Heart (left ventricle)
Acvrl1 mRNA level (2-ΔΔCt)
Eng mRNA level (2-ΔΔCt)
Bmpr2 mRNA level (2-ΔΔCt)
Id1 mRNA level (2-ΔΔCt)
Smad6 mRNA level (2-ΔΔCt)
WT
Bmp9-KO
Bmp10-cKO
DKO
*
e
WT
Bmp9-KO
Bmp10-cKO
DKO
pSmad 1/5/8
β-actin
60 kDa
42 kDa
pSmad 2/3
pSmad 1/5/8 : β-actin ratio (AU)
pSmad 2/3 : β-actin ratio (AU)
**
****

Figure S5

a

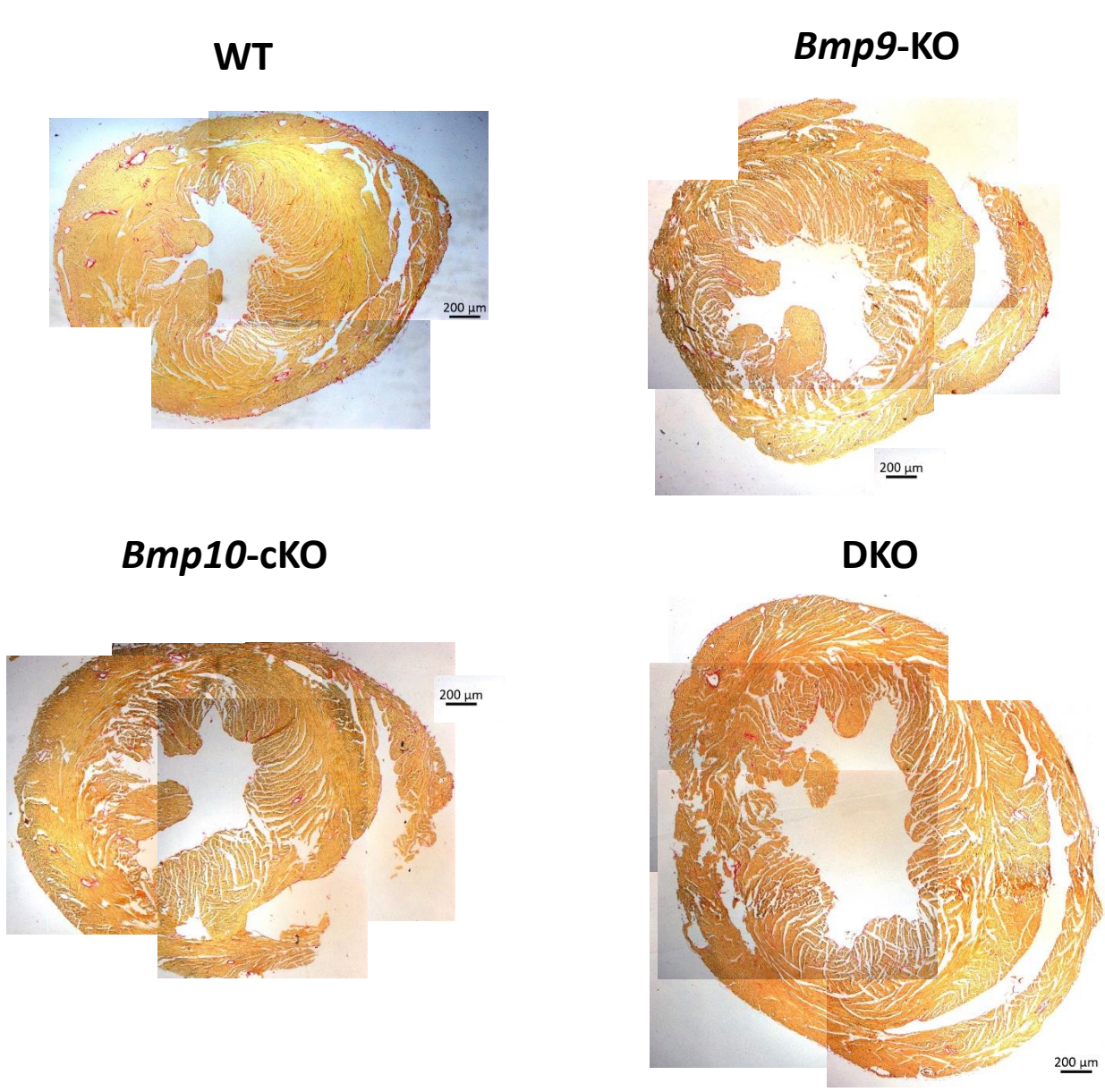
WT
Bmp9-KO
Bmp10-cKO
DKO
200 µm
200 µm
200 µm
200 µm

b

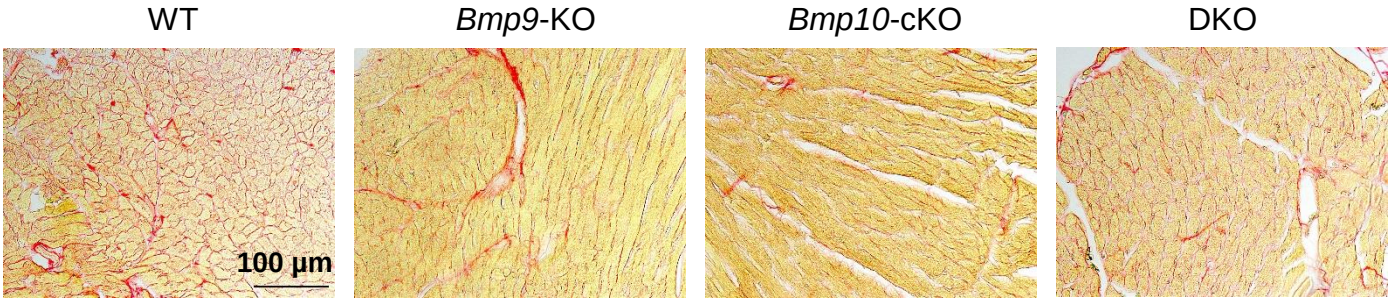
WT
Bmp9-KO
Bmp10-cKO
DKO
100 µm

Figure S6

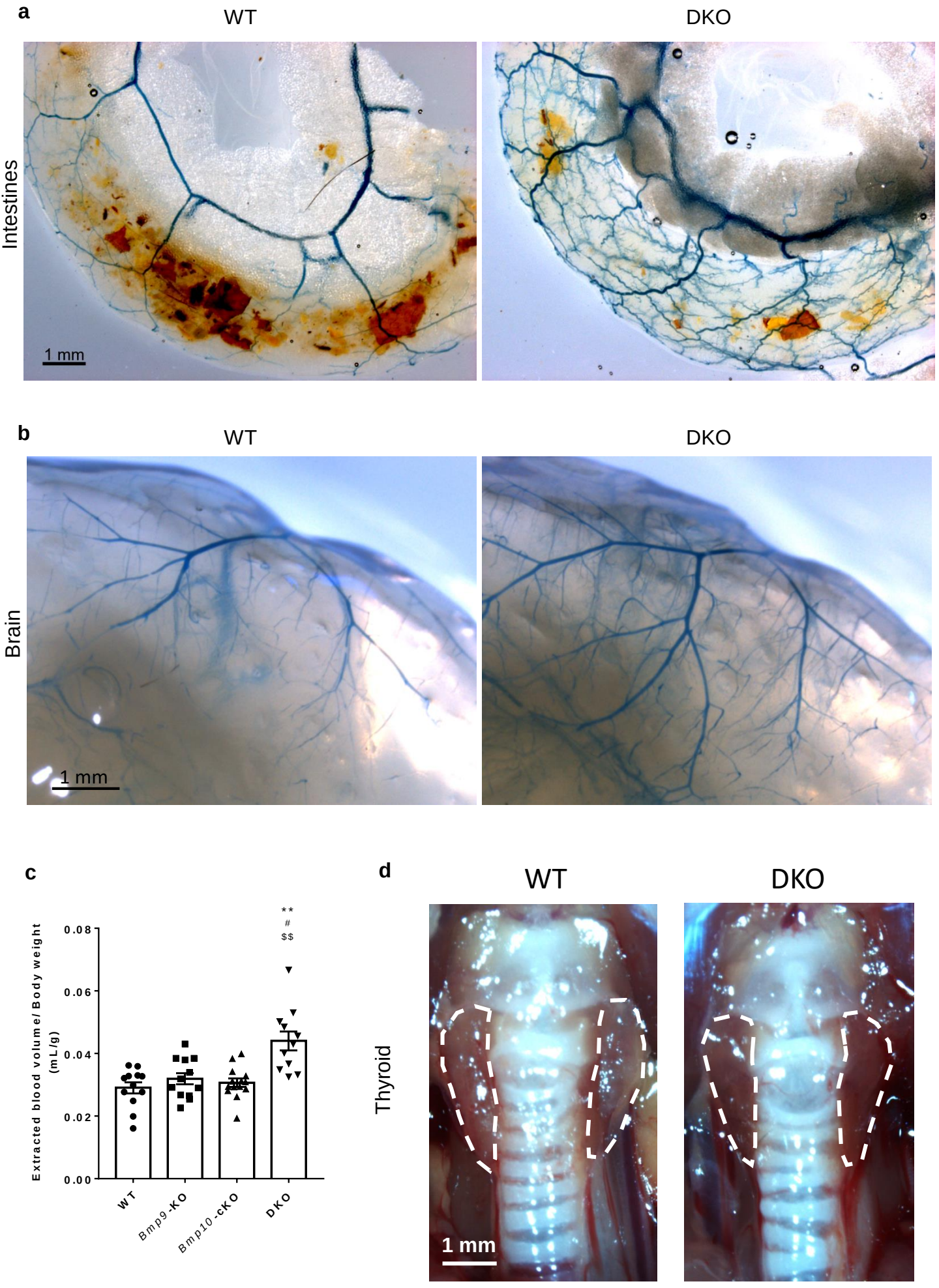
a
WT
DKO
Intestines
1 mm
b
WT
DKO
Brain
1 mm
c
Extracted blood volume/ Body weight (mL/g)
0.08
0.06
0.04
0.02
0.00
**
#
$$
WT
Bmp9-KO
Bmp10-cKO
DKO
d
WT
DKO
Thyroid
1 mm

Figure S7

Gene Ontology Biological Process : top20

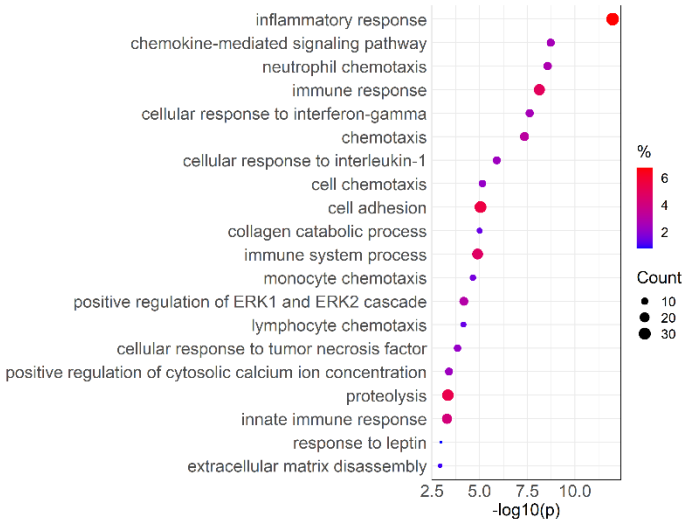

Gene Ontology Biological Process : selection

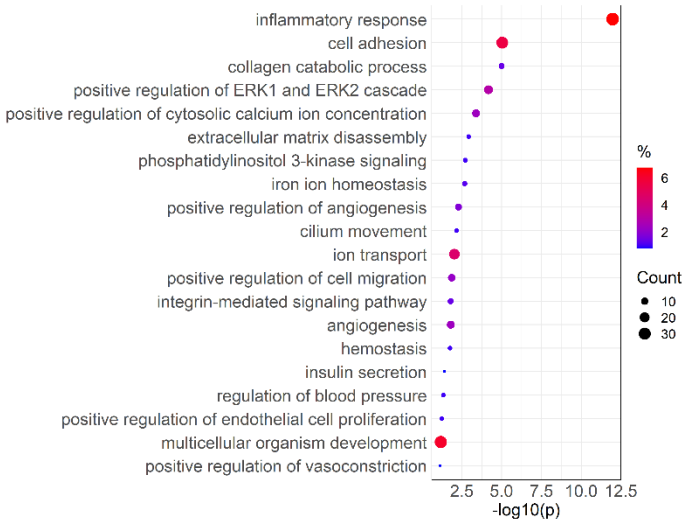

Gene Ontology Molecular Function : top20

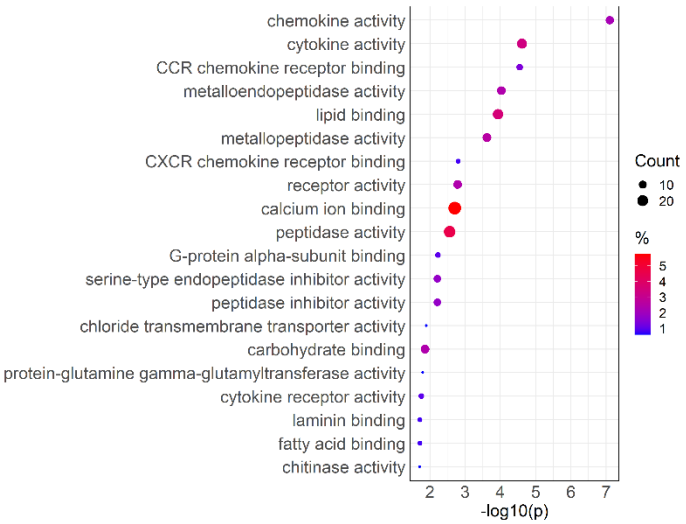

Gene Ontology Cellular Component : top20

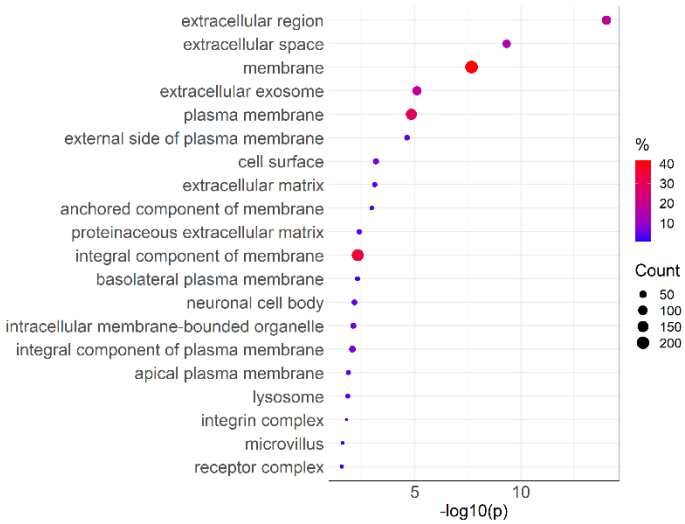

KEGG

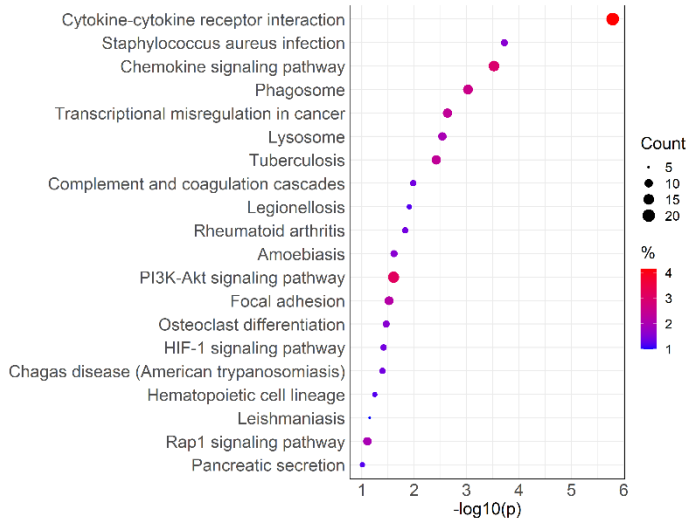

Figure S8

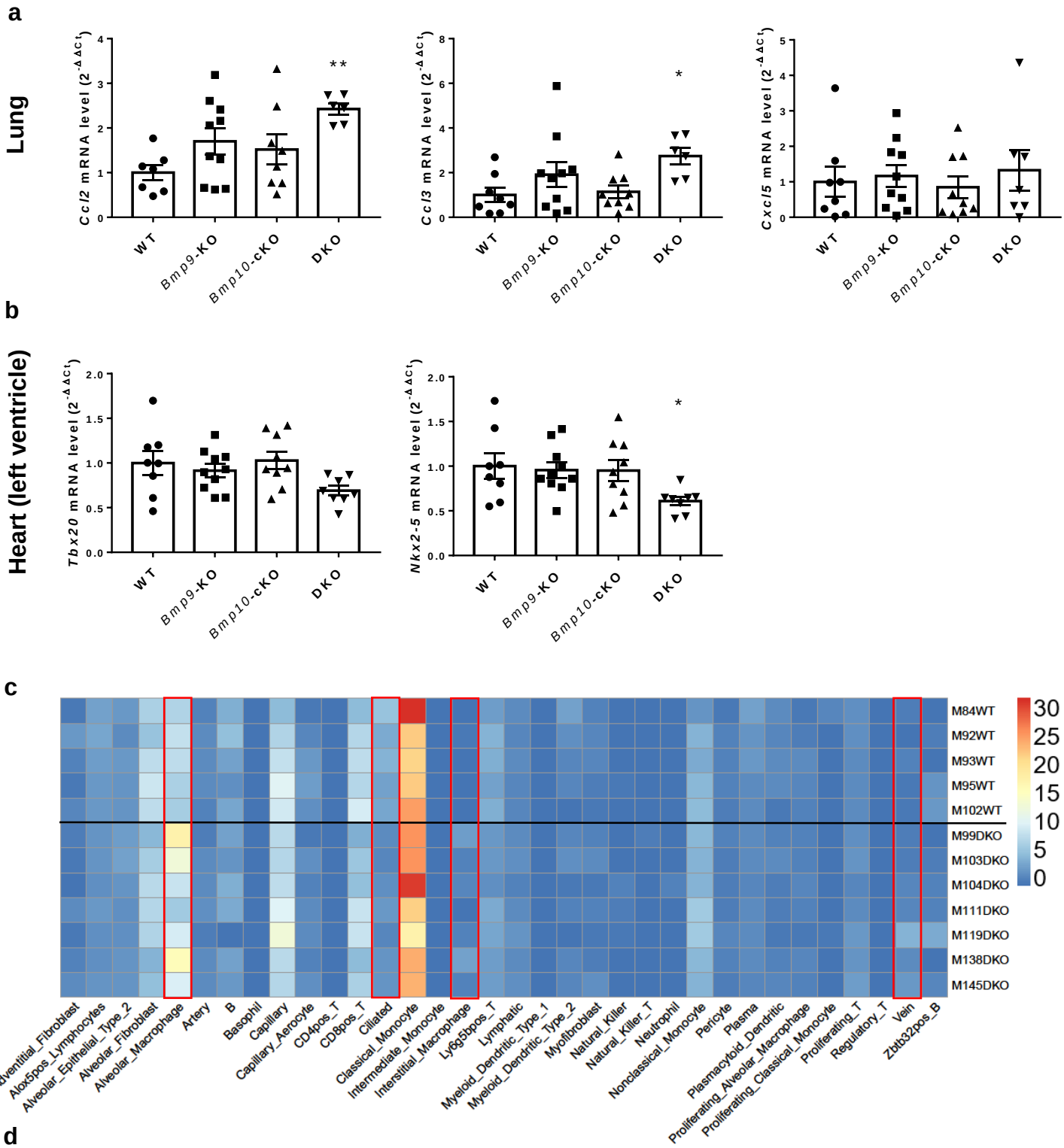
a
Lung
Ccl2 mRNA level (2-ΔΔCt)
Ccl3 mRNA level (2-ΔΔCt)
Cxcl5 mRNA level (2-ΔΔCt)
WT
Bmp9-KO
Bmp10-cKO
DKO
b
Heart (left ventricle)
Tbx20 mRNA level (2-ΔΔCt)
Nkx2-5 mRNA level (2-ΔΔCt)
c
M84WT
M92WT
M93WT
M95WT
M102WT
M99DKO
M103DKO
M104DKO
M111DKO
M119DKO
M138DKO
M145DKO
Adventitial_Fibroblast
Alox5pos_Lymphocytes
Alveolar_Epithelial_Type_2
Alveolar_Fibroblast
Alveolar_Macrophage
Artery
B
Basophil
Capillary
Capillary_Aerocyte
CD4pos_T
CD8pos_T
Ciliated
Classical_Monocyte
Intermediate_Monocyte
Interstitial_Macrophage
Ly6g5bpos_T
Lymphatic
Myeloid_Dendritic_Type_1
Myeloid_Dendritic_Type_2
Myofibroblast
Natural_Killer
Natural_Killer_T
Neutrophil
Nonclassical_Monocyte
Pericyte
Plasma
Plasmacytoid_Dendritic
Proliferating_Alveolar_Macrophage
Proliferating_Classical_Monocyte
Proliferating_T
Regulatory_T
Vein
Zbtb32pos_B
d
Alveolar macrophages (%)
Interstitial macrophages (%)
Vein (%)
Ciliated (%)

Figure S9

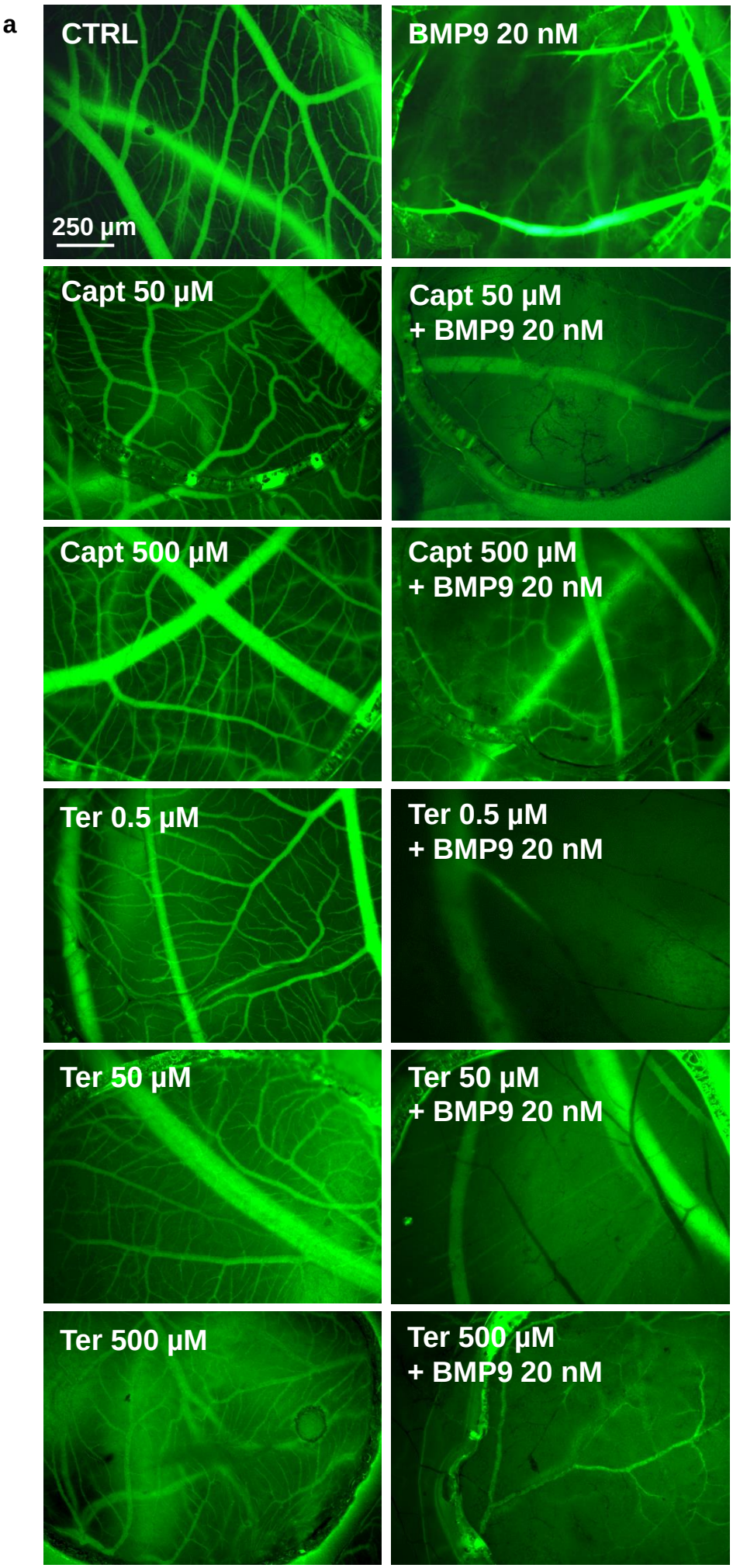
a
CTRL
BMP9 20 nM
250 µm
Capt 50 µM
Capt 50 µM
+ BMP9 20 nM
Capt 500 µM
Capt 500 µM
+ BMP9 20 nM
Ter 0.5 µM
Ter 0.5 µM
+ BMP9 20 nM
Ter 50 µM
Ter 50 µM
+ BMP9 20 nM
Ter 500 µM
Ter 500 µM
+ BMP9 20 nM

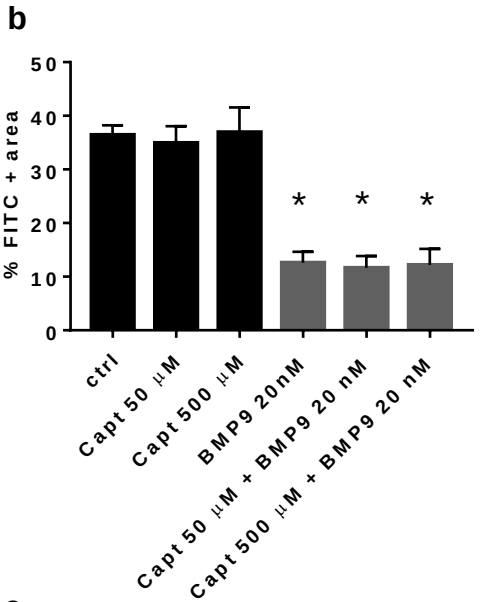
b
% FITC + area
0
10
20
30
40
50
*
*
*
ctrl
Capt 50 µM
Capt 500 µM
BMP9 20nM
Capt 50 µM + BMP9 20 nM
Capt 500 µM + BMP9 20 nM

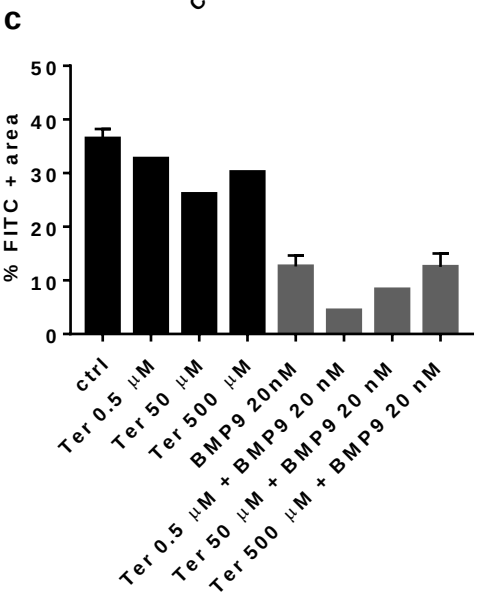
c
% FITC + area
0
10
20
30
40
50
ctrl
Ter 0.5 µM
Ter 50 µM
Ter 500 µM
BMP9 20nM
Ter 0.5 µM + BMP9 20 nM
Ter 50 µM + BMP9 20 nM
Ter 500 µM + BMP9 20 nM